

The continuum limit of f_B from the lattice in the static approximation.

C.R. Allton

*INFN, Sezione di Roma and Dipartimento di Fisica,
Universita di Roma 'La Sapienza', P.le A. Moro, I-00185 Rome, Italy.*

Abstract

We present an analysis of the continuum extrapolation of f_B in the static approximation from lattice data. The method described here aims to uncover the systematic effects which enter in this extrapolation and has not been described before. Our conclusions are that we see statistical evidence for scaling of f_B^{stat} for inverse lattice spacings $\gtrsim 2$ GeV but not for $\lesssim 2$ GeV. We observe a lack of *asymptotic* scaling for a variety of quantities, including f_B^{stat} , at all energy scales considered. This can be associated with finite lattice spacing systematics. Once these effects are taken into account, we obtain a value of 230(35) MeV for f_B^{stat} in the continuum where the error represents uncertainties due to both the statistics and the continuum extrapolation. In this method there is no error due to uncertainties in the renormalization constant connecting the lattice and continuum effective theories.

1 Introduction

The decay constant of the B -meson, f_B , defined through the matrix element of the axial current, A_μ ,

$$\langle 0|A_\mu|B(p) \rangle \equiv if_B p_\mu \quad (1)$$

(where $B(p)$ is a B -meson of momentum p), is an essential ingredient in many calculations in the Standard Model of Particle Physics. For example, it enters in the theoretical determinations of (i) the mass splitting in the $B-\bar{B}$ system, which is proportional to the square of f_B and, in principle, (ii) the Cabibbo-Kobayashi-Maskawa matrix element, V_{ub} , and hence, through the unitary triangle to the element V_{td} (see eg. [1]). Clearly therefore, for a more complete knowledge of some of the fundamental parameters of the Standard Model, theorists need to provide a prediction of f_B (see also [2]).

The two main methods of determining f_B from theory are QCD Sum Rules (see eg. [3]) and Lattice Gauge Theory (see eg. [4, 5]). The QCD Sum Rules has an important advantage compared to the lattice in that it is an analytic, rather than a numerical method. However it involves approximations to the full theory that cannot be systematically improved, and it has a perturbative component calculated at a momentum scale $\mu \approx 1$ GeV where the validity of perturbation theory can be questioned.

In contrast to QCD Sum Rules, the lattice is a fully non-perturbative approach and furthermore uses approximations that can be systematically improved. For each approximation there is an associated *tunable* “lattice parameter” which can eventually be adjusted towards its physical value thereby removing the approximation. For example, lattice calculations are performed on a finite physical volume which can, in principle, be increased towards the physical value (ie. infinity) such that finite volume effects can be neglected to within any desired accuracy. In general the size of the systematic errors introduced due to these lattice approximations has been quantified and often does not present a problem given the size of the statistical errors. This is particularly true in the following analysis.

A lattice approximation that warrants further discussion is the “Quenched Approximation” where the effects of sea quark loops are suppressed. All the lattice results discussed here were obtained using the quenched approximation. There is, however, strong circumstantial evidence that its effects on hadronic masses are small and its effects on hadronic matrix elements are of the level of the statistical errors (10% – 20%) [6]. There will be a further discussion on quenching in the final section.

The reason that these lattice parameters are not set to their physical values in the first place is due to the limitations of present computing power. In this sense, with the inevitable development of computing resources, lattice QCD results will

be able to provide predictions with ever increasing precision.

Turning to the determination of f_B , there is one immediate, technical problem in simulating a b -quark on the lattice: its mass is larger than the ultraviolet cut-off provided by the finite spatial resolution of the lattice, ie. $m_b > a^{-1}$. Here a^{-1} , the inverse lattice spacing, is typically of order 1–3 GeV in present simulations. There are two approaches to overcome this problem. One is to study quarks which are fairly heavy, but whose masses are still less than a^{-1} and then to extrapolate to m_b , and the second is to use the “static approximation” which is the leading term in the heavy quark expansion [7]¹. This paper deals with lattice results using this second approach. To obtain the real value of f_B (ie. to all orders in the heavy quark expansion), one must interpolate results from the two approaches [8].

Historically, lattice calculations of f_B^{stat} (ie. f_B in the static approximation), have proved very difficult due to the low signal to noise ratio of the hadronic correlators required for the calculation [9]. The first successful measurements [10, 11] produced surprisingly large values, $f_B^{stat} \approx 300$ MeV. Since then, many calculations, *at the same value of a* , have generally confirmed these early measurements [12]–[19]. However when calculations at different values of a were performed there appeared, in some analyses, to be a trend towards smaller values of f_B^{stat} as $a \rightarrow 0$, ie. as the “lattice parameter”, a , is tuned towards its physical value [5, 12, 13]. The requirement for lattice results at a non-zero value of a to be physically relevant is that physical quantities remain a constant in the continuum limit, $a \rightarrow 0$, ie. that they *scale*². This apparent downward trend of f_B^{stat} , if actually present, is therefore a violation of scaling and is to be contrasted with the apparent scaling behaviour observed in other physical quantities [20]. It must be stressed that, statements regarding scaling or the lack of it can only be made within a certain statistical uncertainty, and for quantities as difficult to determine as f_B^{stat} , these errors are typically large. At some point scaling violations may disappear below the level of statistics, and hence become unimportant.

The issue of scaling is normally studied by plotting the ratios of physical quantities as a function of a , as was the case in the above-mentioned analyses of f_B^{stat} in which an apparent violation of scaling was observed. This paper outlines an alternative method of studying scaling behaviour in which the functional form of the dimensionless lattice quantity corresponding to f_B^{stat} , (ie. Z_L , defined later in eq.(10)), is fitted as a function of the bare lattice coupling. We show that this analysis applied to the currently published data on f_B^{stat} shows that its scaling violations for $a^{-1} \gtrsim 2$ GeV are small, ie. that they have fallen to below the statistical errors. However, for $a^{-1} \lesssim 2$ GeV we do find scaling violations. This

¹The static approximation will be discussed in more detail in the next section.

²This nomenclature is in analogy with critical phenomena where all physical quantities are proportional to the correlation length raised to a scaling index.

suggests that the conclusions of the studies [5, 12, 13] are due to the inclusion of data too far from the continuum, ie. with $a^{-1} < 2$ GeV. The implication of this result is that, at present, the best estimate for the continuum value of f_B^{stat} is given by those simulations at $a^{-1} \approx 2 - 3$ GeV.

In the following section we outline the static theory as applied on the lattice. Those readers familiar with the static theory on the lattice may wish to skip this section. In sec.3 we study the scaling of f_B^{stat} and other physical quantities, and in sec.4 we discuss our results. We also investigate finite lattice spacing, or $O(a)$, effects and the approach to asymptotic scaling. Once these issues are studied and understood we obtain a continuum value for f_B^{stat} of 230(35) MeV.

2 Static theory on the lattice

This section begins with a brief description of the lattice method of calculating physical quantities. For a full discussion see, for example, the review articles [4, 21].

Lattice QCD typically studies Euclidean correlation functions, $C(t)$, of hadronic operators O^L ,

$$C(t) = \langle O^L(t) O^L(0) \rangle. \quad (2)$$

For purposes of explanation, we will define

$$O^L(t) = \sum_{\tilde{x}} A_0(\tilde{x}, t) = \sum_{\tilde{x}} \psi_1(\tilde{x}, t) \gamma_0 \gamma_5 \psi_2(\tilde{x}, t), \quad (3)$$

where the $\gamma_{0,5}$ are Dirac spinor matrices, and the subscripts 1, 2 are flavour indices. At large times t , $C(t)$ has the following behaviour:

$$C(t) \rightarrow \frac{|\langle 0|O^L|P \rangle|^2}{2M_P^L} e^{-M_P^L t} \quad (4)$$

where P is the lowest state with the quantum numbers of O^L , in our case a pseudo-scalar meson. Once the exponential behaviour in eq.(4) has been established, a simple exponential fit provides lattice predictions of the decay constant,

$$f_P^L = \langle 0|O^L|P \rangle / M_P^L, \quad (5)$$

(cf. eq.(1)) and the mass, M_P^L . We will refer to these lattice predictions, f_P^L and M_P^L , generically as Ω_i^L (whether they be hadron masses or matrix elements). These are not physical quantities because (i) all the fields in the lattice action are made dimensionless using the lattice spacing a , and therefore all the predictions, Ω_i^L , from the lattice are also dimensionless, and, (ii) in the case of matrix elements, the operator O^L , is not correctly normalized.

To determine the scale a we choose a lattice prediction of *one* physical quantity and compare it to the experimental (dimensionful) value, Ω_i . The lattice operator O^L is correctly normalized to its continuum counterpart O typically through a multiplicative renormalization factor Z^{Ren} , ie. $O = Z^{Ren} O^L$ (see eg. [22]). Combining both steps we have:

$$a_i^{-1} = \frac{\Omega_i}{Z_i^{Ren} \Omega_i^L}. \quad (6)$$

(In this discussion we are assuming that Ω_i has energy dimension unity.) For non-matrix element quantities such as hadron masses M^L , $Z^{Ren} \equiv 1$.

In lattice QCD, we have dimensional transmutation in action: we first set the bare coupling in the lattice action, g^2 , at the start of the calculation, and then determine the corresponding ultraviolet cutoff, a^{-1} , through eq.(6). (We could instead proceed in the reverse direction, by first setting a^{-1} , but this would require expensive simulations at many trial values of g^2 before we settled at the correct value of g^2 corresponding to the chosen value of a^{-1} .)

Finally then we have the lattice prediction of a dimensionful physical quantity, Ω_j :

$$\begin{aligned} \Omega_j &= Z_j^{Ren} \Omega_j^L a_i^{-1} \\ &= \Omega_i \frac{Z_j^{Ren} \Omega_j^L}{Z_i^{Ren} \Omega_i^L} \end{aligned} \quad (7)$$

The correlation function $C(t)$ is numerically calculated using the Wick contracted form of eq.(2),

$$C(t) = \langle Tr\{G_1(t, 0)\gamma_0\gamma_5 G_2(0, t)\gamma_0\gamma_5\} \rangle. \quad (8)$$

The quark propagators $G_{1,2}$ are defined from the lattice version of the Dirac equation.

In the static version of the theory G_1 is defined using the solution of the Dirac equation in the limit of an infinitely heavy quark (see eq.(2.37) in [4]). In this case we are simulating a pseudo-scalar meson (which we'll denote B) made up of a light quark and an infinitely heavy quark. We have from eqs.(1,4),

$$C(t) \rightarrow \frac{(f_B^{stat,L})^2 M_B a}{2} e^{-E_B t}, \quad (9)$$

where E_B is the binding energy³ of the light quark in the B-meson, and M_B is the experimental value of the B -meson mass. We define

$$Z_L^2 \equiv (\Omega_{f_B}^L)^2 = \frac{(f_B^{stat,L})^2 M_B a}{2}. \quad (10)$$

³ We have factored out the exponential time dependence of the (infinitely-heavy) quark in the static propagator.

This is the lattice quantity corresponding to f_B^{stat} (see sec.1). Note that in [12] the symbol \tilde{f}_B is used for Z_L . Correctly normalizing the operator, and putting in the appropriate dimensions (cf. eq.(7)) we have,

$$f_B^{stat} = \sqrt{\frac{2}{M_B}} Z_{f_B}^{Ren} Z_L a^{-3/2}. \quad (11)$$

The issue of scaling is then simply a question of whether the g^2 dependences of the $Z_{f_B}^{Ren}$, Z_L and $a^{-3/2}$ cancel in eq.(11).

Using eq.(6) we have finally

$$f_B^{stat} = \sqrt{\frac{2 \Omega_i^3}{M_B}} \frac{Z_{f_B}^{Ren} Z_L}{(Z_i^{Ren} \Omega_i^L)^{3/2}}. \quad (12)$$

3 Continuum scaling of f_B^{stat}

The usual method of determining whether the scaling⁴ region of a lattice simulation has been reached is to study a dimensionless ratio, $\frac{\Omega_1}{\Omega_2}$, of physical quantities Ω_i , to see if this ratio is a constant in a , or equivalently in g^2 . Using eq.(7) the Ω_i in the ratio can be replaced with the dimensionless quantity $Z_i^{Ren} \Omega_i^L$. Dimensionless ratios of lattice quantities are generally used wherever possible because statistical fluctuations, and indeed, some systematic effects tend to cancel. For this reason ratios are often better determined than the absolute quantities themselves.

Using this ‘‘ratio’’ method, we show in fig.(1) the plot of f_B^{stat} versus a_σ , ie. the lattice spacing determined from the string tension σ . The data plotted is a collection of published data on f_B^{stat} and is reported in table 1 with references cited in column 1. (Note that $\beta = 6/g^2$, where g is the bare lattice coupling which appears in the lattice action.) For completeness, in table 1, we also list the values of $Z_{f_B}^{Ren}$ and a^{-1} used and the f_B^{stat} obtained by each group. In the figure we use eq.(12) to determine the f_B^{stat} values given the Z_L values in table 1. The $Z_{f_B}^{Ren}$ values we have used are the boosted, tadpole improved values [23, 24], which means, for instance, at $\beta = 6.0$ we have $Z_{f_B}^{Ren} = 0.70$ for the Wilson action, and 0.79 for the clover action.

It is difficult to interpret this plot, and difficult to gauge the likelihood of a decrease or increase of f_B^{stat} as $a \rightarrow 0$. Of course, one can simply use a linear or quadratic fit [4, 5, 12, 13], and fit the data in any case. The problem with this approach is that continuum value of f_B^{stat} in fig.(1) is the extrapolation of the ratio of two quantities (in this case Z_L and $(\Omega_\sigma^L)^{3/2}$, see eq.(12)) which have *very similar* functional dependencies on a . Any slight systematic effect in either the

⁴ as opposed to *asymptotic* scaling - see sec.4

numerator or denominator will swing the ratio, which therefore could significantly affect the extrapolation.

In this paper we show that such a systematic effect is present in the form of scaling violations for $a^{-1} \lesssim 2$ GeV. In the approach presented here, the functional dependence of the numerator and denominator are determined separately, and then compared to check for scaling. We then present a method which does not suffer from the above problem and enables a continuum estimate of f_B^{stat} to be made.

We begin by assuming a naive scaling of the Ω^L quantity appropriate for f_B^{stat} , ie. Z_L (see eq.(10))

$$Z_L \sim e^{-9S_{f_B}/g^2}. \quad (13)$$

We will justify this choice of functional behaviour in the next section and show that, for our purposes, there is no loss of generality in eq.(13). Assuming this relationship, we now plot in fig.(2) $\log(Z_L)$ against $1/g^2$. Later we will fit this plot to a straight line to extract S_{f_B} ⁵. We notice immediately from fig.(2) that the data fall in a roughly linear band, and with a relatively small spread. One could imagine using this plot to check future calculations of Z_L at smaller a values. It is obvious that the behaviour of Z_L with g^2 apparent in fig.(2) is more clearly manifest than the behaviour of f_B^{stat} with a (see fig.(1)).

We now determine S_{f_B} from the slope of $\log(Z_L)$ against $1/g^2$. For the Wilson data, we choose two intervals: $5.7 \leq \beta \leq 6.0$ and $6.0 \leq \beta \leq 6.3$. The motivation for these two intervals is that there is evidently a dependence of S_{f_B} on g^2 . This will be discussed in detail in the next section. We obtain the values reported in the third column of table 2. For the clover data, we choose the interval $6.0 \leq \beta \leq 6.2$ since the f_B^{stat} data is available only at $\beta = 6.0$ & 6.2 .

Of course, the values of Z_L and their scaling with g^2 are not enough to determine the scaling of f_B^{stat} itself. One needs to also study the g^2 behaviour of some Ω_i^L in order to set the scale. Four such choices are $\sqrt{\sigma}$, M_ρ , f_π , and the $1P - 1S$ splitting in charmonium. In tables 3 & 4, a sample of the published data on a^{-1} from various collaborations is presented with the references cited in column 1. Note that for $a_{f_\pi}^{-1}$, we have used the renormalization constants shown in the tables. Specifically these were obtained with the ‘‘boosted’’ perturbation theory⁶ in the Wilson case [23], and the non-perturbatively obtained values in the clover case [27, 28].

⁵Note that for ease of presentation, we have plotted Z_L values obtained with both Wilson and clover [25] actions together on the same plot. A priori, we cannot expect the same value of S_{f_B} from both actions, so in the determinations of S_{f_B} we fit results from the two actions separately.

⁶In this case we choose the ‘‘boosted’’ coupling $g_V^2 = g^2/u_0^4$ where u_0^4 is the average plaquette, see [23].

Ref.	Action	$\beta = 6/g^2$	Z_L	a^{-1}	Z^{Ren}	f_B^{stat} MeV
[10] - ELC	Wilson	6.0	0.22(2)	2.0(2) ^b	0.8 ^g	310(25)(50)
[13] - WPC	Wilson	5.74	0.543(20)	1.119(8) ^e		
[13] - WPC	Wilson	6.0	0.231(10)	1.88(2) ^e		
[13] - WPC	Wilson	6.26	0.125(8)	2.78(2) ^e		
[12] - FNAL	Wilson	5.7	0.564(28)	1.15(8) ^f	0.63 ^h	271(13)(20)
[12] - FNAL	Wilson	5.9	0.250(14)	1.78(9) ^f	0.65 ^h	241(13)(13)
[12] - FNAL	Wilson	6.1	0.135(13)	2.43(15) ^f	0.68 ^h	215(21)(14)
[12] - FNAL	Wilson	6.3	0.099(8)	3.08(18) ^c	0.68 ^h	225(17)(14)
[14] - BLS	Wilson	6.3	0.094(6)	3.21(9)(17) ^d	0.7 ^h	235(20)(21)
[16] - UKQCD	clover	6.0	0.211 ⁺⁶ ₋₇	2.0 ^{+3b} ₋₂	0.78 ⁱ	286 ⁺⁸⁺⁶⁷ ₋₁₀₋₄₂
[16] -UKQCD	clover	6.2	0.117 ⁺⁷ ₋₇	2.7 ^{+7b} ₋₁	0.79 ⁱ	253 ⁺¹⁶⁺¹⁰⁵ ₋₁₅₋₁₄
[17] - Ken	Wilson	6.0	0.184(7) ^a	2.0	0.70 ^h	224 ⁺⁹ ₋₇
[18] - APE	Wilson	6.0	0.23(3)	2.11(5)(10) ^b	0.8 ^g	350(40)(30)
[18] - APE	clover	6.0	0.23(3)	2.05(6) ^b	0.89 ^g	370(40)
[19] - APE	clover	6.2	0.111(6)	3.0(3) ^b	0.81 ^h	290(15)(45)

Table 1: Values for Z_L and f_B^{stat} from various group's work.

^a this Z_L value was obtained from eq.(11), ie. the Z_L value was not explicitly published

^b a^{-1} from averaging scale obtained from f_π and M_ρ

^c a^{-1} from the 1P-1S value at $\beta = 6.1$ using 1-loop asymptotic freedom to extrapolate to $\beta = 6.3$

^d a^{-1} from f_π

^e a^{-1} from the string tension, σ

^f a^{-1} from $1P - 1S$ charmonium splitting

^g Z^{Ren} from standard perturbative result

^h Z^{Ren} from boosted, tadpole improved analysis

ⁱ Z^{Ren} from boosted analysis

<i>Action</i>	<i>Fitting interval</i>	S_{f_B}	S_σ	S_{M_ρ}	S_{f_π}	S_{1P-1S}
Wilson	$5.7 \leq \beta \leq 6.0$	2.39(10)	2.06(3)	1.53(7)	1.8(2)	2.2(4)
	$6.0 \leq \beta \leq 6.3$	1.57(11)	1.52(6)	1.35(13)	1.7(2)	—
Clover	$6.0 \leq \beta \leq 6.2$	2.1(2)	1.52(6)	1.7(2)	2.1(3)	—

Table 2: Values for S_i obtained from fits to the data in tables 1, 3 and 4 to eqs.(13,14). Note $\beta = 6/g^2$.

Again we assume the data to have the following functional form (see eg. [8]):

$$a_i = \frac{Z_i^{Ren} \Omega_i^L}{\Omega_i} \sim e^{-6S_i/g^2} \quad (14)$$

where $i = \sigma, M_\rho, f_\pi, 1P - 1S$, and we have used eq.(6). As in eq.(13), this functional form can be assumed with no loss of generality.

In figs.(3-6), $\log(a_i)$ is plotted against $1/g^2$ for the Wilson data from table 3. From the gradient of this plot fitted in the same intervals as the fit of $\log(Z_L)$, we obtain the values of S_i , $i = \{\sigma, M_\rho, f_\pi, 1P - 1S\}$ reported in table 2.

We now turn to a discussion of the continuum limit of f_B^{stat} . The functional behaviour of f_B^{stat} , using eqs.(11,13,14) is:

$$f_B^{stat}(g^2) \sim \frac{Z_L}{a_i^{3/2}} = e^{-9(S_{f_B} - S_i)/g^2}. \quad (15)$$

We have ignored the g^2 dependence of the renormalization constant $Z_{f_B}^{Ren}$, and will justify this below. Thus, the issue of scaling is addressed in this analysis by a comparison of S_{f_B} and S_i . We believe this is a cleaner method of studying the scaling of f_B^{stat} since the systematics present in both Z_L and a_i^{-1} can be isolated and studied.

From table 2 for $\beta = 6/g^2 \leq 6.0$ there is a clear statistical evidence for a *violation* of scaling in the Wilson data, ie. the S_i are not all compatible.

For $6.0 \leq \beta \leq 6.3$, in the Wilson case, all the S_i are within around one standard deviation of the value 1.5. In fact both the S_σ and S_{f_π} values in table 2 are probably a little too high because there is no a_σ^{-1} or $a_{f_\pi}^{-1}$ data in this range above $\beta = 6.2$. The conclusion is therefore that $f_B^{stat}, \sigma, M_\rho, f_\pi$ and $1P - 1S$ mutually scale within present statistical errors for $a^{-1} \gtrsim 2$ GeV. This is the main

Ref.	$\beta = 6/g^2$	a_σ^{-1}	$a_{M_\rho}^{-1}$	$a_{f_\pi}^{-1}$	$Z_{f_\pi}^{Ren}$	a_{1P-1S}^{-1}
[13] - WPC	5.7	1.025(3)				
[26] - FNAL	5.7					1.15(8)
[6] - GF11	5.7		1.42(2)	1.25(5)	0.75	
[13] - WPC	5.74		1.44(3)			
[13] - WPC	5.8	1.272(6)				
[13] - WPC	5.9	1.55(2)				
[26] - FNAL	5.9					1.78(9)
[6] - GF11	5.93		1.99(4)	2.00(5)	0.77	
[13] - WPC	6.0	1.88(2)	2.25(10)			
[18] - APE	6.0		2.23(5)	2.21(8)	0.78	
[29] - APE	6.0		2.18(9)	1.97(8)	0.78	
[26] - FNAL	6.1					2.43(15)
[6] - GF11	6.17		2.77(4)	2.82(7)	0.79	
[13] - WPC	6.2	2.55(1)				
[29] - APE	6.2		2.88(24)	2.96(24)	0.79	
[13] - WPC	6.26		3.69(32)			
[13] - WPC	6.4	3.38(1)				
[8] - ELC	6.4		3.70(15)	4.0(6)	0.80	

Table 3: Values for a^{-1} obtained from various group's work using the Wilson action.

Ref.	$\beta = 6/g^2$	$a_{M_\rho}^{-1}$	$a_{f_\pi}^{-1}$	$Z_{f_\pi}^{Ren}$
[18] - APE	6.0	2.05(6)	2.11(11)	1.09(3)
[30] - APE	6.0	1.92(11)	1.94(5)	1.09(3)
[31] - APE	6.0	1.95(7)	1.78(9)	1.09(3)
[16] - UKQCD	6.2	2.7(1)	3.2(2)	1.04(1)
[19] - APE	6.2	3.05(19)	2.73(17)	1.04(1)

Table 4: Values for a^{-1} obtained from various group's work using the Clover action.

result of this paper. Results which suggest a decrease of f_B^{stat} as $a \rightarrow 0$ can now be understood to be due to the inclusion of $\beta < 6.0$ data which suffer from systematic effects due to the lack of scaling of the quantities involved.

In the clover case, there exists only two collaboration's results, and at only two β values, and so an interpretation of the results, in this case, may be premature. To elaborate, if the UKQCD results [16] are not included in the determination of the S_i , we obtain the following values:

$$S_{f_B} = 2.1(2), \quad S_{M_\rho} = 2.1(3), \quad S_{f_\pi} = 1.7(3), \quad (16)$$

to be compared with the values in the last row of table 2. Evidently the S_{M_ρ} and S_{f_π} values interchange when the UKQCD results are not included. This suggests that more results, particularly at larger β are required to settle the S_i values in the clover case. In any case, the results suggest that f_B^{stat} , M_ρ and f_π mutually scale also in the clover case (for $\beta \gtrsim 6.0$).

4 Discussion

In the rest of the paper asymptotic scaling, lattice artefacts and the continuum value of f_B^{stat} will be discussed.

Asymptotic scaling is where the g^2 dependence of lattice quantities Ω_i^L is the same as that predicted by weak-coupling perturbation theory. This behaviour can be obtained by integrating the beta-function of the theory,

$$\beta(g^2) = a \frac{dg^2}{da} = 2\beta_0 \frac{g^4}{16\pi^2} + 2\beta_1 \frac{g^6}{(16\pi^2)^2} + O(g^8), \quad (17)$$

to obtain,

$$a = \Lambda^{-1} f_{PT}(g^2), \quad (18)$$

where

$$f_{PT} = (g^2)^{\frac{-\beta_1}{2\beta_0^2}} e^{-\frac{16\pi^2}{2\beta_0} \frac{1}{g^2}}, \quad (19)$$

$\beta_{0,1}$ are given by:

$$\beta_0 = \frac{(11N - 2n_f)}{3}, \quad \beta_1 = \frac{34}{3}N^2 - \frac{10}{3}Nn_f - \frac{(N^2 - 1)}{N}n_f, \quad (20)$$

n_f is the number of flavours, N the number of colours and Λ is some constant of integration. The subscript “ PT ” refers quantities obtained from (second-order) weak-coupling perturbation theory. For the quenched theory⁷, $n_f = 0$, so we have from eq.(14)

$$S_{PT} = \frac{1}{6} \frac{16\pi^2}{22} \approx 1.20, \quad (21)$$

⁷see eg. [32] for a discussion of asymptotic scaling in the unquenched theory

where we have ignored higher order terms (ie. set $\beta_1 = 0$). We expect, for small enough g^2 , that $S_i = S_{PT}$. From table 2 we see that this is not the case. In the following, we discuss the possible causes for this discrepancy.

4.1 Effects of higher order terms

The first and most obvious explanation for the inequality, $S_i \neq S_{PT}$, is that for the values of g^2 in table 2, the effect of higher order terms (β_1, β_2, \dots) is significant. Note moreover that the downward trend of the S_i towards S_{PT} as g^2 decreases is at least consistent with the prediction of weak-coupling perturbation theory and the declining importance of the higher order corrections in this limit.

However, to study this hypothesis quantitatively, we first note that from eq.(11), the lattice prediction of f_B^{stat} is given by:

$$f_B^{stat} \sim Z_{f_B}^{Ren}(g^2) Z_L(g^2) (g^2)^{\frac{3\beta_1}{4\beta_0^2}} e^{9S_{PT}/g^2}, \quad (22)$$

where we have assumed the two-loop formula (eq.(18)) for a , and have included a g^2 dependence in Z^{Ren} . $Z_{f_B}^{Ren}$ has the following expansion in g^2 :

$$Z_{f_B}^{Ren}(g^2) = 1 - \epsilon g^2 + O(g^4), \quad (23)$$

where $\epsilon \approx 0.2$. In this formula we have taken only the matching between the lattice and continuum effective theories and have ignored the anomalous dimension [33] (see also [12]). It can easily be demonstrated that this extra factor does not affect the following discussion.

Since f_B^{stat} is a fixed physical number, we have, using eqs.(13, 22 & 23)

$$Z_L(g^2) \sim (1 + \epsilon g^2) (g^2)^{\frac{-3\beta_1}{4\beta_0^2}} e^{-9S_{PT}/g^2} \sim e^{-9S_{f_B}(g^2)/g^2} \quad (24)$$

where we've now allowed for a g^2 dependence in S_{f_B} . Solving eq.(24) for $S_{f_B}(g^2)$, using the fact that ϵ is small, we obtain:

$$S_{f_B}(g^2) \approx S_{PT} - \frac{\beta_1}{12\beta_0^2} g^2 + \frac{\epsilon}{9} g^4. \quad (25)$$

Thus for $\epsilon \approx 0.2$ we get

$$S_{f_B}(g^2) \approx 1.20 - 0.07g^2 + 0.02g^4, \quad (26)$$

which is not compatible with the values in table 2. More significantly, eq.(26) does not explain the strong dependence of S_{f_B} on the g^2 interval (see table 2) or even the fact that $S_i > S_{PT}$. Thus this analysis suggests that higher order effects cannot explain the lack of asymptotic scaling of f_B^{stat} (ie. $S_{f_B} \neq S_{PT}$) in

<i>Fitting interval</i>	S_σ^V	S^V from eq.(27)
$5.7 \leq \beta \leq 6.0$	1.39(2)	1.07
$6.0 \leq \beta \leq 6.3$	1.26(5)	1.09

Table 5: Values for S^V obtained from (i) fits to the string tension data in table 3 to eq.(14), but with $g \rightarrow g_V$ (column 2), and, (ii) a theoretical evaluation using eq.(27) (column 3).

table 2. A similar analysis of the affects of the higher order terms in S_i , $i = \{\sigma, M_\rho, f_\pi, 1P - 1S\}$ leads to the same conclusion. The only difference in these cases is that the definition of the S_i in eq.(14) includes the Z_i^{Ren} factor, whereas the definition of S_{f_B} in eq.(13) does not.

The derivation of $S_{f_B}(g^2)$ leading to eq.(25) proves the statements above which stated that the functional form chosen in eqs.(13,14) is quite general for our purposes. Any g^2 dependence in eg. Z^{Ren} can be factored into the definition of S_i . It is also appropriate to note here that the contribution of Z^{Ren} to $S_{f_B}(g^2)$ is $\approx \epsilon/9 \lesssim 0.03$ which is much smaller than the typical statistical errors present in $S_{f_B}(g^2)$ in table 2. This justifies ignoring the g^2 dependence of $Z_{f_B}^{Ren}$ in eq.(15).

Recently, effects due to higher order terms in lattice perturbation theory have been addressed [23]. In this work, it has been suggested that g , the coupling constant appearing in the lattice action, is a poor choice of expansion parameter and the use of a “boosted” coupling, g_V , was advocated. A typical choice of g_V is $g_V^2 \approx g^2/u_0^4$, where u_0^4 is the average plaquette. A straightforward fit of a_σ as in eq.(14), but with g replaced by g_V , leads to the values of S_σ^V in table 5, column 2.

A theoretical evaluation based on that leading to eq.(25), but with g replaced with g_V gives the result:

$$\begin{aligned}
S^V(g_V^2) &\approx S_{PT} - \frac{\beta_1}{12\beta_0^2} g_V^2 \\
&\approx 1.20 - 0.07g_V^2.
\end{aligned}
\tag{27}$$

ϵ does not appear in eq.(27) since it is zero for the string tension (ie. $Z_\sigma^{Ren} \equiv 1$). The values obtained from this formula are shown in the last column of table 5. Again, the theoretical predictions do not match the results from the data. Also it is significant that the trend of S_σ^V with g^2 cannot be reproduced, even with a boosted coupling.

We do not choose to fit the data for $a_{M_\rho, f_\pi, 1P-1S}^{-1}$ to the boosted asymptotic

scaling prediction since the larger errors in these cases make the conclusive interpretation of results difficult.

4.2 Lattice Artefacts

The above discussion on higher order terms is an entirely continuum issue - it does not include any effect which is purely lattice in origin. In the following we discuss artefacts of the lattice formulation. Recalling the discussion in the introduction, we list the “lattice parameters” that are involved in these calculations⁸: $\{ m_q, L, \text{Quenching}, a(g^2) \}$, where m_q is the (light-) quark mass and L is the physical extent of the lattice in fermi. We discuss the effects of each of these parameters in the following to try to determine the cause of the observed lack of asymptotic scaling.

“ m_q ” effects

The lattice values of f_B^{stat} in this study are all the values obtained after an extrapolation in the light quark mass, m_q , to zero. Thus there is no problem associated with the light-quark mass not being adjusted to its physical value. One may, however, worry about a systematic error due to the extrapolation in m_q ⁹. This is unlikely to cause a problem since the dependence on m_q of Z_L and indeed M_ρ, f_π , and many other quantities is mild (see eg. table 3 in [19]). Presumably also, any systematic effect associated with m_q does not depend greatly on g^2 over the range studied in this analysis.

Finite Volume effects

The effects of finite L on many physical observables has been extensively studied [6, 13, 35]. For example, within present statistics, for $L \gtrsim 1.5fm$, f_B^{stat} is not a function of L [13]. This bound is not entirely satisfied by all the data in this analysis. So to study this explicitly, we take the Z_L values from table 1 at $\beta = 6.0$ and plot them in fig.(7) as a function of the L used for each simulation. There appears if anything to be a *decrease* in Z_L , and therefore correspondingly f_B^{stat} , as L increases, and this is contrary to the observed behaviour [13] (see also [15]). For this reason, and because generally speaking, different g^2 values in table 1 have their lattice sizes chosen such that $L \approx const$, we do not believe that finite volume effects are to blame for S_i not being equal to its asymptotic

⁸ In the past there was concern that f_B^{stat} may also be dependant on the “smearing” size of the interpolation operator used to extract the matrix element [34]. However, it is now clear that it is not the case [4, 5, 12, 13, 18].

⁹Normally simulations are performed with $m_q \gtrsim 100 \text{ MeV} \gg m_{u,d}$.

freedom value, S_{PT} .

Quenching

The numerical effects of quenching on lattice calculations are normally difficult to uncover, but in the case of S_i this is not the case. To see this we note that the quenched approximation is really an effective theory of QCD where the sea quark loops are totally neglected and the coupling, g^2 , is adjusted to try to compensate for these missing interactions. In an ideal world, this adjustment would be perfect, and predictions from the correctly-adjusted quenched theory would match those of the unquenched theory. However, due to the complicated structure of the interactions, this is presumably not the case! This means that, for example, instead of using the experimental (ie. unquenched) value of $\Omega_{M_\rho} = M_\rho = 770$ MeV to set a_{M_ρ} , we should use the value of M_ρ in a world without sea quark loops but where other physical quantities (such as σ etc.) were as close as possible to their experimental values in our unquenched world. That is we should use

$$a_{M_\rho}^{-1} = \frac{M_\rho^{\text{Quenched-World}}}{M_\rho^L} \quad (28)$$

cf. eq.(6). The difference between this prescription and the usual one (where instead of $M_\rho^{\text{Quenched-world}}$ we have $M_\rho = 770$ MeV) is simply a constant pre-factor, independent of g^2 , and therefore this cannot affect S_{M_ρ} .

“O(a)-Effects”

The final lattice artefact to be discussed is that due to the finiteness of the lattice parameter a . These so-called “ $O(a)$ ” effects have long been studied (see eg. [25, 36]) and are known to play an important role in matrix element calculations [27, 37]. They arise because the standard Wilson action replaces continuum derivatives by finite differences over nearest neighbours and is thus equal to the continuum action only up to $O(a)$. The clover action is improved to the extent that its predictions are correct to $O(a/\log(a))$ [37]. (Note that the static theory on the lattice is also correct to this order [38].) The pure gauge sector of both lattice actions is correct to $O(a^2)$, and therefore the string tension, which is a pure gauge quantity, is correct to this order.

Summarizing this discussion, we have for the Wilson case:

$$\Omega_i^L = \Omega_i^{PL} + O(a), \quad (29)$$

and for the clover case:

$$\Omega_i^L = \Omega_i^{PL} + O(a/\log(a)), \quad (30)$$

where $i = f_B, M_\rho, f_\pi, 1P - 1S$, and for the pure gauge case:

$$\Omega_\sigma^L = \Omega_\sigma^{PL} + O(a^2). \quad (31)$$

The Ω_i^{PL} are the results that would be obtained with a perfect lattice action, ie. one correct to all orders in a . Using eqs.(29 & 31) together with eqs.(6 & 18), we obtain, in the Wilson case for $i = M_\rho, f_\pi, 1P - 1S$,

$$a_i^{-1}(g^2) = \Lambda_i f_{PT}^{-1}(g^2) \left(1 - X_i \frac{f_{PT}(g^2)}{f_{PT}(1)}\right), \quad (32)$$

and, for $i = \sigma$,

$$a_\sigma^{-1}(g^2) = \Lambda_\sigma f_{PT}^{-1}(g^2) \left(1 - X_\sigma \left(\frac{f_{PT}(g^2)}{f_{PT}(1)}\right)^2\right), \quad (33)$$

where X_i is the relative strength of the $O(a)$ (or $O(a^2)$) correction at $g^2 = 1$, ie. $\beta = 6/g^2 = 6.0$. Here we have replaced a_{PL} with $\Lambda^{-1} f_{PT}$ (see eq.(18)) since $a_{PL} = \Lambda^{-1} f_{PT}$ up to exponentially suppressed non-perturbative pieces.

Thus we see straightaway that in the limit where the effects of quenching are unimportant (and therefore $\Lambda_i = \Lambda_j$) $a_i^{-1}(g^2) - a_j^{-1}(g^2) = const.$ for fermionic Wilson quantities. In the future, with better statistics, this can be checked.

We are now in a position to fit the data in table 3 to the appropriate eqs.(32 & 33). In this fit there are two free parameters: X_i and the coefficient, Λ_i .

Taking all the $a_\sigma^{-1}(g^2)$ values in table 3 and fitting them to eq.(33) we obtain $X_\sigma = 0.197(2)$ with a χ^2/dof of 11/4 which is shown in table 6. As a check we also fit $a_\sigma^{-1}(g^2)$ to eq.(32) obtaining, as expected, a poorer χ^2/dof of 26/4 with $X_\sigma = 0.343(4)$. This suggests that we are in fact isolating the $O(a^2)$ corrections in $\sqrt{\sigma}$, and that furthermore, the largish value of χ^2/dof in the fit to eq.(33) may signal the statistical presence of even higher order terms (ie. of $O(a^n), n > 2$). The fit of $a_\sigma^{-1}(g^2)$ to eq.(33) is shown in fig.(8) as a solid line. In this figure we have also shown, as a dashed curve, a fit to the 2-loop asymptotic scaling formulae with the boosted coupling g_V as discussed in sec.4.1 (ie. eq.(18) with $g^2 \rightarrow g_V^2 = g^2/u_0^4$, where u_0^4 is the average plaquette). As can be seen from fig.(8), the quality of this boosted asymptotic scaling fit is poor; in fact the χ^2/dof for this fit is around 10^3 . On the other hand, the fit to eq.(33) (ie. the asymptotic scaling formulae with an $O(a^2)$ term) is very acceptable. This suggests strongly that the observed lack of asymptotic scaling in the string tension data can be simply explained by $O(a^2)$ -effects.

i	σ	M_ρ	f_π	1P-1S
fit to eq.	33	32	32	32
X_i	0.197(2)	0.21(2)	0.31(5)	0.35(11)
Λ_i (MeV)	1.780(5)	2.12(6)	2.4(1)	2.5(3)
χ_i^2/dof	11/4	8/8	8/5	0.3/1

Table 6: Values for X_i , Λ_i and χ^2/dof obtained from fits of the Wilson data in table 3 to eqs.(32,33) as indicated.

In the case of $a_{M_\rho, f_\pi, 1P-1S}^{-1}$ for the Wilson data, a fit to eq.(32) gives the values for Λ_i and X_i shown in table 6. These fits are shown in figs.(9-11). Again the χ^2/dof are very acceptable.

Due to the quality of the fits we conclude that the most satisfactory explanation of the observed lack of *asymptotic* scaling (ie. $S_{\sigma, M_\rho, f_\pi, 1P-1S} \neq S_{PT}$) is $O(a)$ effects. This is the only explanation out of those discussed here which seems consistent with the data.

The results for the Λ values in table 6 indicate that Λ_σ is significantly lower than the Wilson values for $\Lambda_{M_\rho, f_\pi, 1P-1S}$, and that therefore results using a_σ^{-1} will differ statistically in the continuum limit from those using $a_{M_\rho, f_\pi, 1P-1S}^{-1}$. However, σ itself is in fact a poorly determined quantity since it relies on model calculations, and furthermore, from above arguments, the low value of Λ_σ may signal the effect of quenching.

For the clover case, we do not attempt to extract the coefficient of the $a/\log(a)$ term due to the fact that there are data at only two values of g^2 available. We await further data before attempting this analysis. Also, we choose not to perform a combined least squares fit of $a_{M_\rho, f_\pi, 1P-1S}^{-1}$ to eq.(32) together with a_σ^{-1} to eq.(33) with a *single* Λ , since quenching implies that a single Λ is inappropriate.

We can continue the analysis of the $O(a)$ effects by fitting Z_L as follows:

$$\frac{1}{Z_L^{2/3}} = \lambda_{Z_L} f_{PT}^{-1}(g^2) \left(1 - X_{Z_L} \frac{f_{PT}(g^2)}{f_{PT}(1)}\right). \quad (34)$$

We obtain the values of X_{Z_L} and λ_{Z_L} in table 7. (Again we have fitted only the Wilson data.) Note that this functional form was chosen to mirror the fits of $a_{\sigma, M_\rho, f_\pi, 1P-1S}^{-1}$ to eqs.(32 & 33). However, of course, in this case the physical value corresponding to Z_L (ie. f_B) is not known, and there is nothing to set the scale; therefore λ_{Z_L} is dimensionless. In fig.(12) we plot the Z_L data against β (for the Wilson action) together with the fit to eq.(34) shown as a solid line. Note from this plot and from the relatively poor χ^2 in table 7 that there appears to be some

fit to eq.	34
X_{Z_L}	0.42(3)
λ_{Z_L}	$3.7(1) \times 10^{-3}$
χ_i^2/dof	39/9

Table 7: Values for X_{Z_L} , λ_{Z_L} and χ^2/dof obtained from a fit of the Z_L values in table 1 to eq.(34).

systematic effects remaining in the data. This is not entirely surprising due to the known difficulty of extracting Z_L .

We are now in a position to obtain a continuum value of f_B^{stat} . Using eqs.(11,32,33,34), in the limit $a \rightarrow 0$

$$f_B^{stat}(a=0) = \sqrt{\frac{2}{M_B}} Z_{f_B}^{Ren}(g^2=0) \left(\frac{\Lambda_i}{\lambda_{Z_L}}\right)^{3/2} \quad (35)$$

where in this limit, $Z_{f_B}^{Ren}(g^2=0) = 1 - \frac{3S_{PT}}{2\pi^2} = 0.82$ We use the average of the $\Lambda_{M_\rho, f_\pi, 1P-1S}$ from table 6 ie. $\Lambda = 2.2(2)$ MeV (where the error is statistical plus systematic combined in quadrature) and obtain,

$$f_B^{stat}(a=0) = 230(35)\text{MeV}. \quad (36)$$

We take this as our best estimate of the continuum value of f_B^{stat} from the lattice. Note that this is roughly equivalent to the values obtained from simulations at finite a values for $a^{-1} \gtrsim 2$ GeV (see fig.(1), note though that this figure uses the scale from the string tension). Had we instead used $\Lambda_\sigma = 1.780(5)$, we would obtain $f_B^{stat}(a=0) = 170(14)$ MeV. We do not prefer to choose this value since it appears that the a_σ^{-1} values are contaminated by either quenched effects, or model dependences.

Since the renormalization constant $Z_{f_B}^{Ren}$ between the lattice and continuum effective theories is evaluated at $g^2 = 0$, it is exactly determined. This is in contrast with the uncertainties in $Z_{f_B}^{Ren}$ at finite g^2 which plague other approaches due to the uncalculated terms of order g^4 and higher.

5 Conclusion

In this paper we have presented a method to obtain the continuum value of f_B^{stat} from lattice data. This approach separately isolates the systematic errors coming from the dimensionless lattice quantity corresponding to f_B^{stat} (ie. Z_L)

and the lattice quantity used to determine the scale. These systematic errors and the lack of asymptotic scaling can be parameterised in terms of finite lattice spacing effects. Assuming this explanation a value of $f_B^{stat} = 230(35)$ MeV in the continuum limit has been obtained. In this method there is no error in the renormalization constant connecting the lattice and continuum effective theories.

6 Acknowledgements

It is a pleasure to thank G. Martinelli and C. Sachrajda for guidance and support over the last years. The author also wishes to acknowledge many useful discussions with colleagues in the APE collaboration, especially M. Crisafulli, V. Lubicz, F. Rapuano and A. Vladikas, and for allowing the use of some unpublished APE data in table 4. We thank the INFN for the financial support which has been forthcoming and the European Union for support under the Human Capital and Mobility Program, contract ERBCHBICT941462.

References

- [1] J. Rosner, in *B Decays*, ed. S.L.Stone, (World Scientific, Singapore 1991).
- [2] M. Ciuchini, E. Franco, G. Martinelli, L. Reina, Phys.Lett. **B301** (1993) 263.
- [3] M. Neubert, SLAC-PUB-6263, June 1993.
- [4] R. Sommer, DESY 94-011, Jan 1994.
- [5] C. Bernard, Nucl.Phys. (Proc.Suppl.) **B34** (1994) 47.
- [6] F. Butler, H. Chen, J. Sexton, A. Vaccarino and D. Weingarten, hep-lat/9405003 and hep-lat/9310009.
- [7] E. Eichten and F. Feinberg, Phys.Rev. **D23** (1981) 2724, M.B. Voloshin and M.A. Shifman, Sov.J.Nucl.Phys. bf 45 (1987) 292, H.D. Politzer and M.B. Wise, Phys.Lett. **206B** (1988) 681, N. Isgur and M. Wise, Phys.Lett. **232B** (1989) 113, Phys.Lett. 237B (1990) 527.
- [8] A. Abada et al, Nucl.Phys. **B376** (1992) 172.
- [9] Ph. Boucaud, O. Pene, V.J. Hill, C.T. Sachrajda and G. Martinelli, Phys.Lett. **B220** (1989) 219.

- [10] C.R. Allton, C.T. Sachrajda, V. Lubicz, L. Maiani and G. Martinelli, Nucl.Phys. **B349** (1991) 598.
- [11] C. Alexandrou et al, Phys.Lett. **B256** (1991) 60.
- [12] A. Duncan et al, Nucl.Phys. (Proc.Suppl.) **B34** (1994) 444, and FERMILAB PUB-94/164-T.
- [13] C. Alexandrou et al, CERN-TH 6692/92, to appear Nucl.Phys.B.
- [14] C.W. Bernard, J.N. Labrenz and A. Soni, UW/PT-93-06, to appear in Phys.Rev.D and Nucl.Phys. (Proc.Suppl.) **B30** (1993) 465.
- [15] C.W. Bernard, J.N. Labrenz and A. Soni, Nucl.Phys. (Proc.Suppl.) **B20** (1991) 488.
- [16] UKQCD Collaboration, R.M. Baxter et al, Phys.Rev. **D49** (1994) 1594.
- [17] T. Draper and C. McNeile, Nucl.Phys. (Proc.Suppl.) **B34** (1994) 453.
- [18] APE Collaboration, C.R. Allton et al., Nucl.Phys. **B413** (1994) 461.
- [19] APE Collaboration, C.R. Allton et al., Phys.Lett. **B326** (1994) 295.
- [20] D. Toussaint, Nucl.Phys. (Proc.Suppl.) **B26** (1992) 3.
- [21] G. Martinelli, Nucl.Phys.B (Proc.Suppl.) 16 (1990) 16, plenary talk at the EPS-High Energy Phys'89, Madrid.
- [22] C.T. Sachrajda, Nucl.Phys. (Proc.Suppl.) **B9** (1989) 121.
- [23] G.P. Lepage and P.B. MacKenzie, Phys.Rev. **D48** (1993) 2250.
- [24] A. Kronfeld, Nucl.Phys. (Proc.Suppl.) **B30** (1993) 445.
- [25] B. Sheikholeslami and R. Wohlert, Nucl.Phys. **B259** (1985) 572.
- [26] A.X. El-Khadra, G.M. Hockney, A.S. Kronfeld and P.B. Mackenzie, Phys.Rev.Lett. **69** (1992) 729.
- [27] G. Martinelli, S. Petrarca, C.T. Sachrajda and A. Vladikas, Phys.Lett. **B311** (1993) 241.
- [28] J. Ivar, G. Martinelli, B. Pendleton, S. Petrarca, C.T. Sachrajda, and A. Vladikas, *unpublished*, see also C.T. Sachrajda, Nucl.Phys. (Proc.Suppl.) **B34** (1994) 507.
- [29] APE Collaboration, talk presented by F. Rapuano, Nucl.Phys. (Proc.Suppl.) **B34** (1994) 360.

- [30] APE Collaboration, talk presented by N. Stella, Nucl.Phys. (Proc.Suppl.) **B34** (1994) 477 (with data updated to 170 configurations).
- [31] APE Collaboration, C.R. Allton et al., *work in progress*.
- [32] G. Cella et al, Phys.Rev. **D49** (1994) 511.
- [33] M.B. Voloshin and M.A. Shifman, Sov.J.Nucl.Phys. **45** (1987) 292; H.D. Politzer and M.B. Wise, Phys.Lett. **B206** (1988) 681, Phys.Lett. **B208** (1988) 504; X. Ji and M.J. Musolf, Phys.Lett. **B257** (1991) 409; D.J. Broadhurst and A.G. Grozin, Phys.Lett. **B267** (1991) 105, Phys.Lett. **B274** (1992) 421; E. Eichten and B. Hill, Phys.Lett. **B234** (1990) 511.
- [34] S. Hashimoto and Y. Saeki, Nucl.Phys. (Proc.Suppl.) **B26** (1992)381.
- [35] C. Alexandrou et al, DESY preprint 93-179.
- [36] K. Symanzik, in *Mathematical problems in theoretical physics*, Springer Lecture Notes in Physics, vol. 153 (1982) 47, eds. R. Schrader, R. Seiler and D.A. Uhlenbrock.
- [37] G. Heatlie, C.T. Sachrajda, G. Martinelli and C. Pittori, Nucl.Phys. **B352** (1991) 266.
- [38] A. Borrelli and C. Pittori, Nucl.Phys. **B385** (1992) 502.

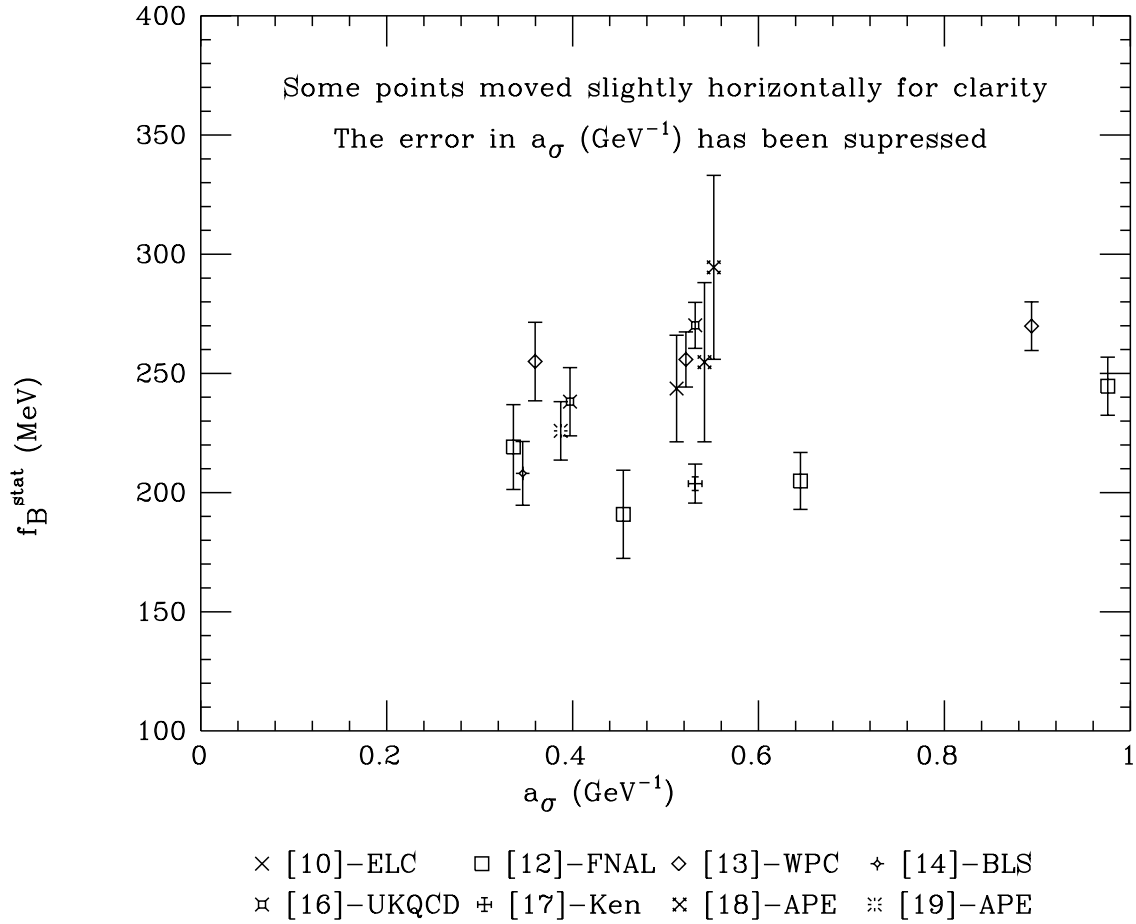


Figure 1: Plot of f_B^{stat} against the lattice spacing as determined from the string tension, a_σ^{-1} , from various groups as listed in the legend. f_B^{stat} has been determined using eq.(11) with $a^{-1} = a_\sigma^{-1}$. See text for the definition of $Z_{f_B}^{\text{Ren}}$ used.

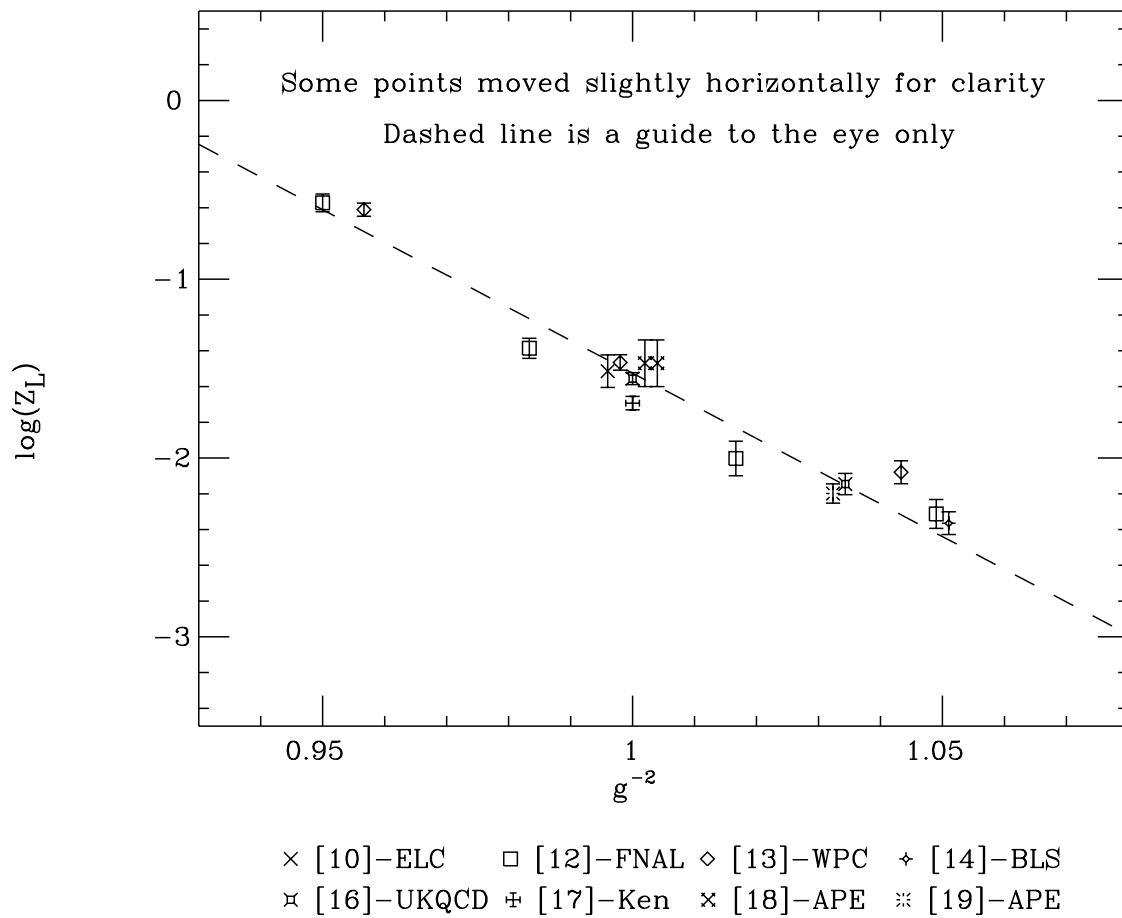


Figure 2: Plot of $\log(Z_L)$ from various groups as listed in the legend. g is the bare lattice coupling.

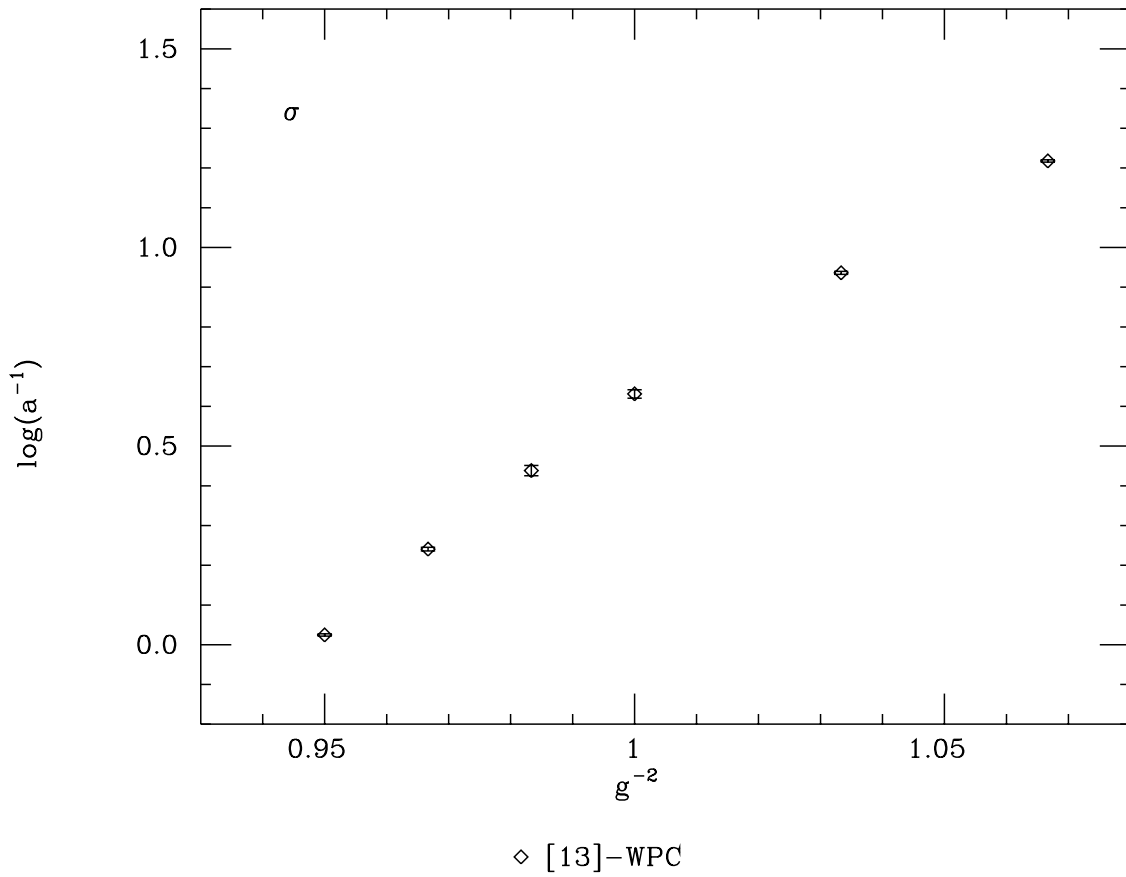


Figure 3: Plot of $\log(a^{-1})$ from the string tension. The reference is as appears in the legend.

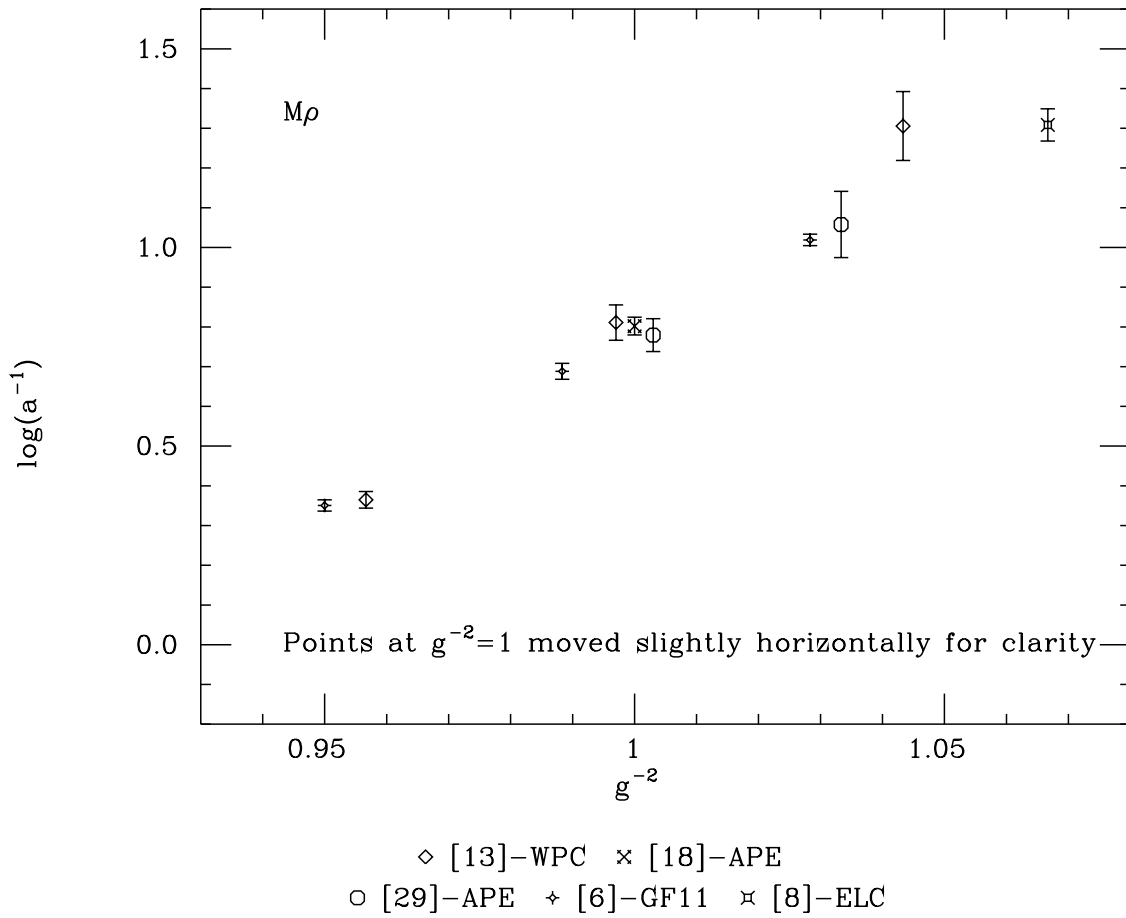


Figure 4: Plot of $\log(a^{-1})$ from M_ρ for the Wilson action. The references are as appears in the legend.

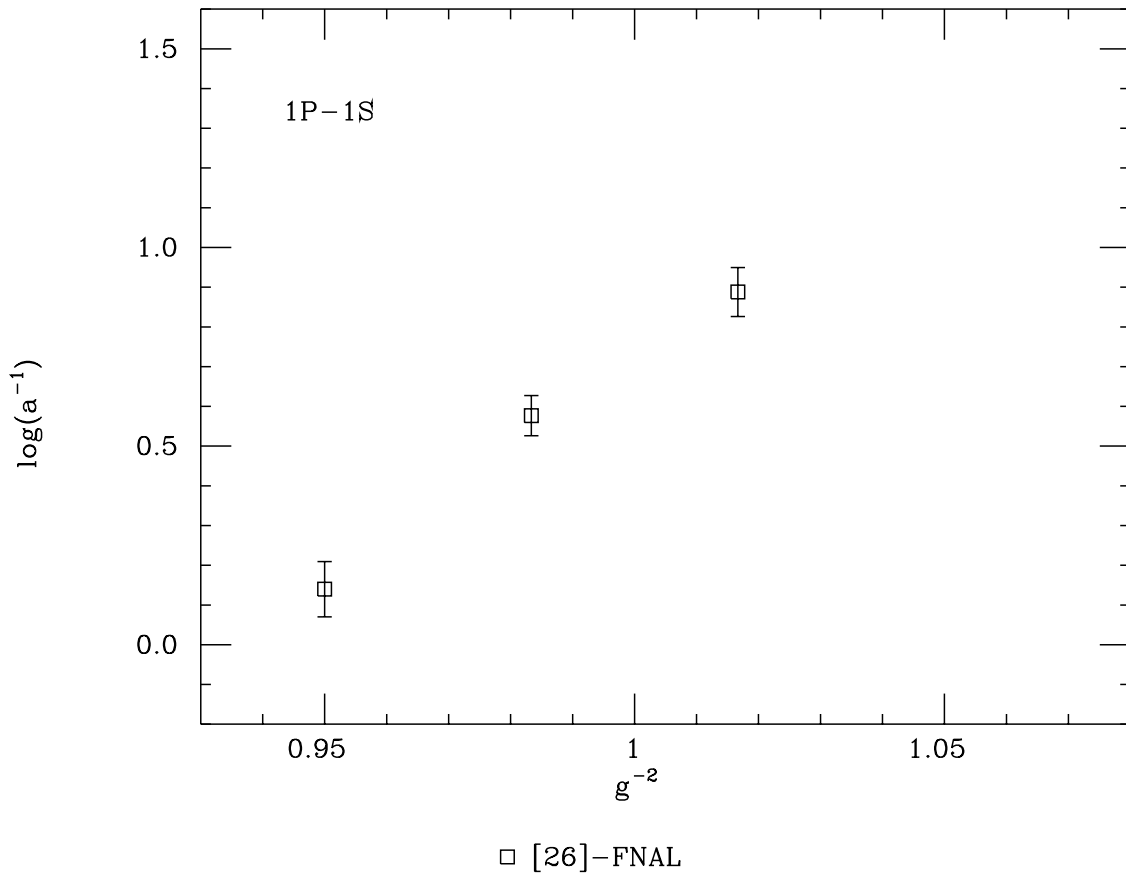


Figure 6: *Plot of $\log(a^{-1})$ from the $1P - 1S$ splitting in charmonium for the Wilson action. The reference is as appears in the legend.*

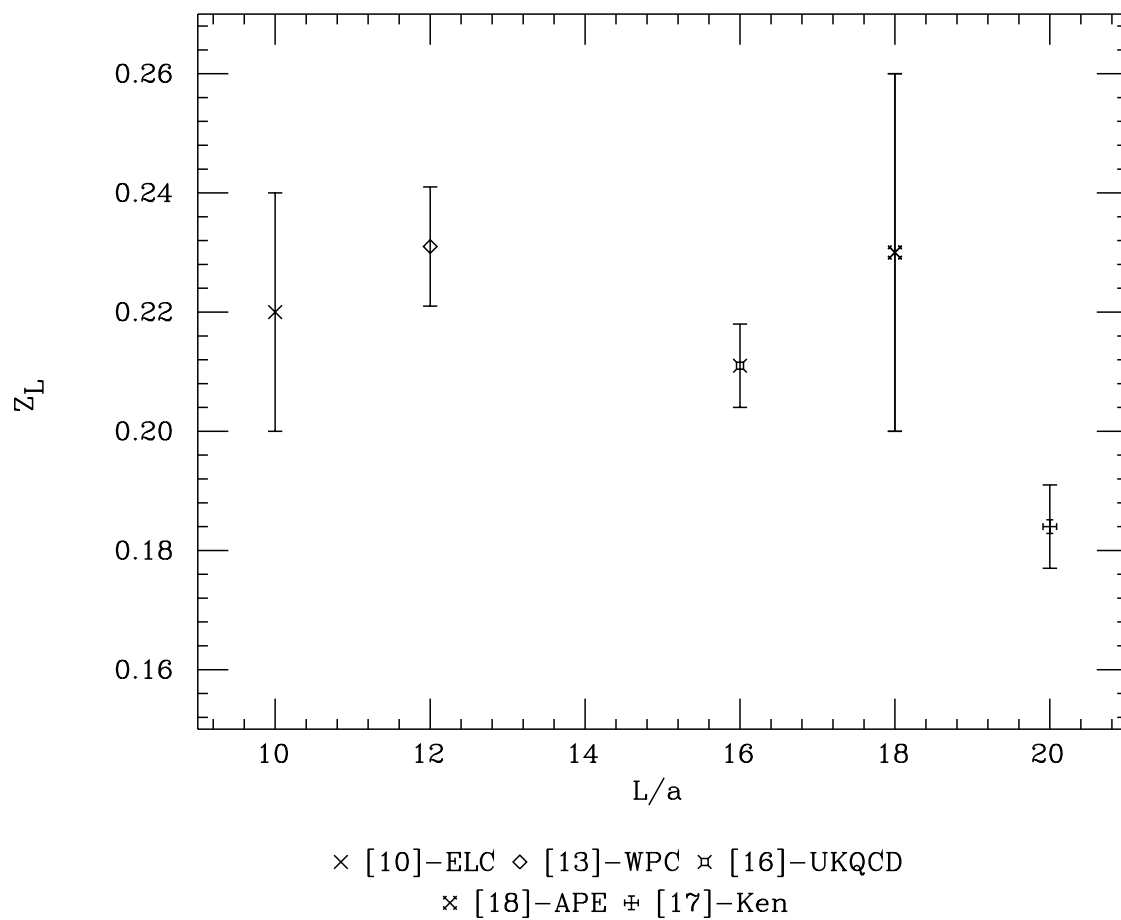


Figure 7: Plot of Z_L from various groups at $\beta = 6/g^2 = 6.0$ against the spatial dimension in lattice units, L/a . The references are as listed in the legend.

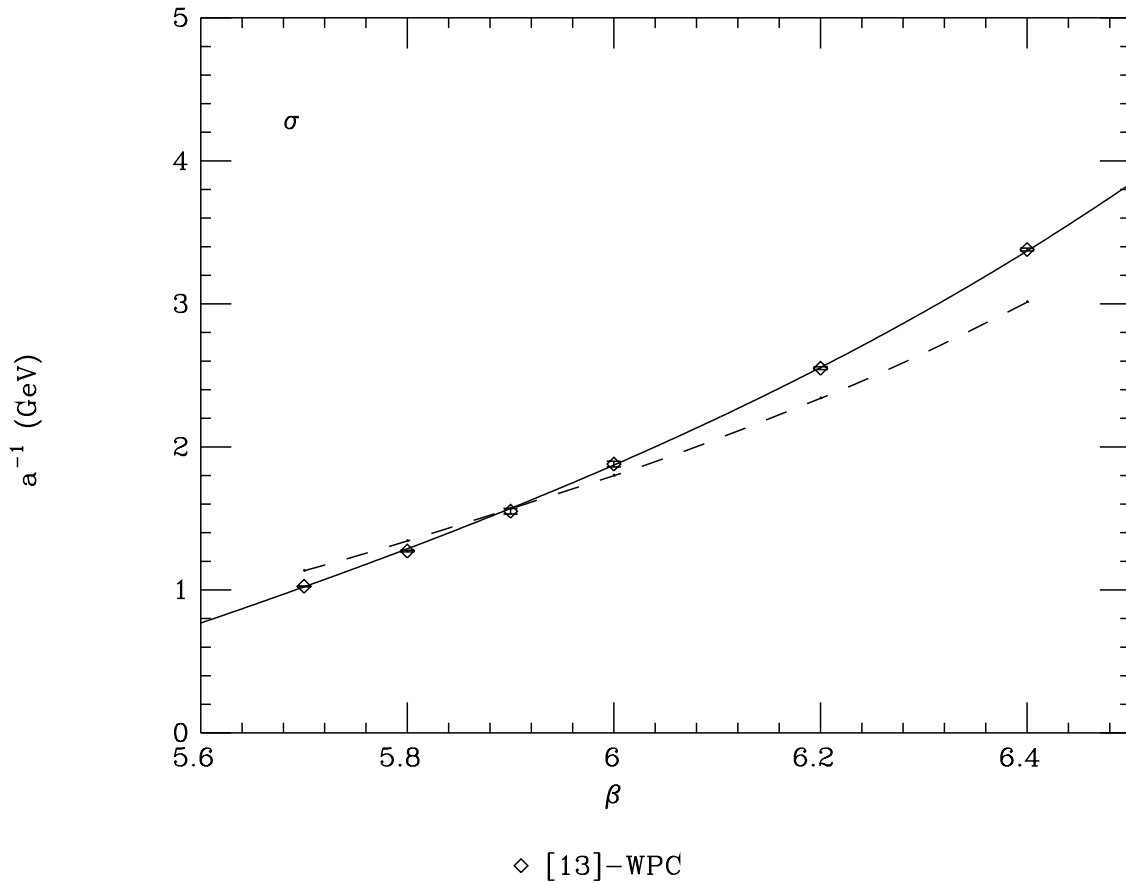


Figure 8: Plot of a^{-1} from the string tension against $\beta = 6/g^2$. The solid curve is the fit to eq.(33) (ie. the 2-loop asymptotic scaling formulae with an $O(a^2)$ term). The dashed curve is the fit to eq.(18) with g^2 replaced by g_V^2 (ie. the “boosted” 2-loop asymptotic scaling formulae). The references are as appears in the legend.

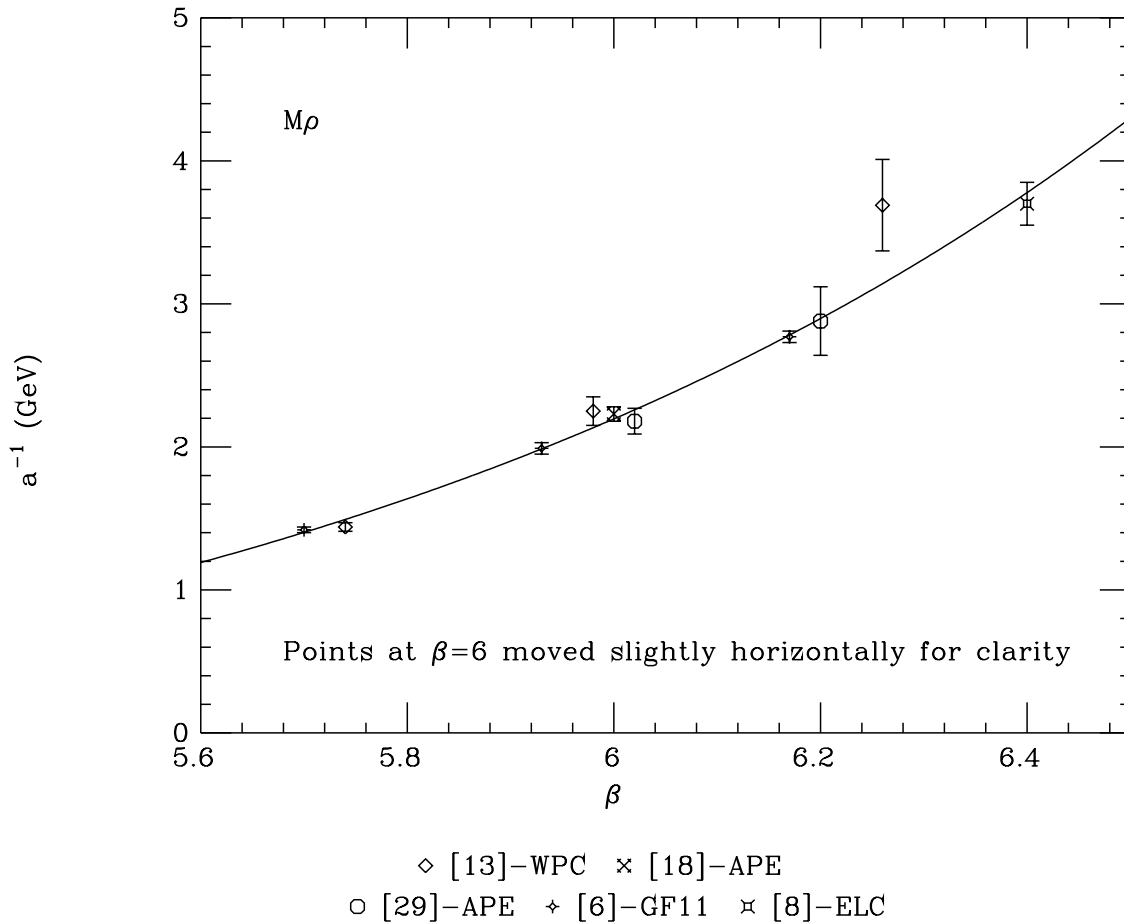


Figure 9: Plot of a^{-1} from M_ρ against $\beta = 6/g^2$. The solid curve is the fit to eq.(32) (ie. the 2-loop asymptotic scaling formulae with an $O(a)$ term). The references are as appears in the legend. All data is from the Wilson action.

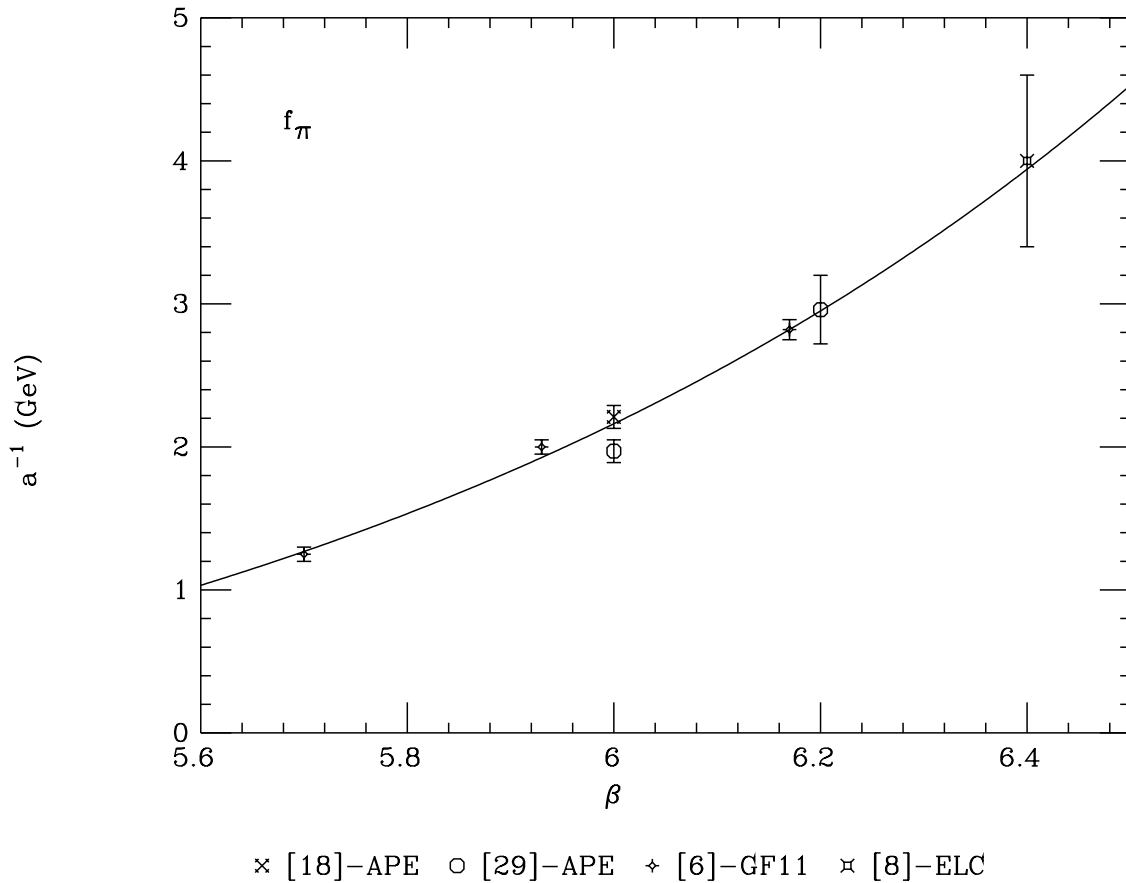


Figure 10: Plot of a^{-1} from f_π against $\beta = 6/g^2$. The solid curve is the fit to eq.(32) (ie. the 2-loop asymptotic scaling formulae with an $O(a)$ term). The references are as appears in the legend. All data is from the Wilson action.

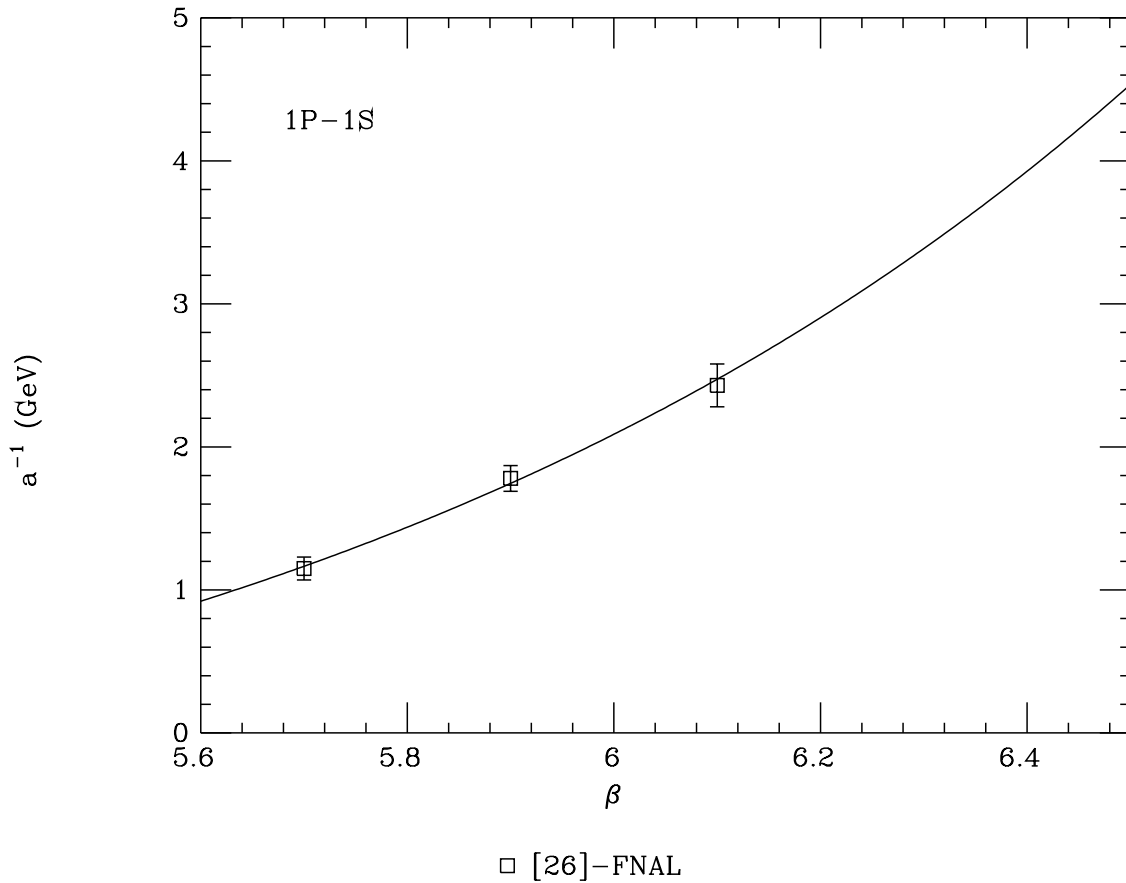


Figure 11: Plot of a^{-1} from the $1P-1S$ splitting in charmonium against $\beta = 6/g^2$. The solid curve is the fit to eq.(32) (ie. the 2-loop asymptotic scaling formulae with an $O(a)$ term). The references are as appears in the legend. All data is from the Wilson action.

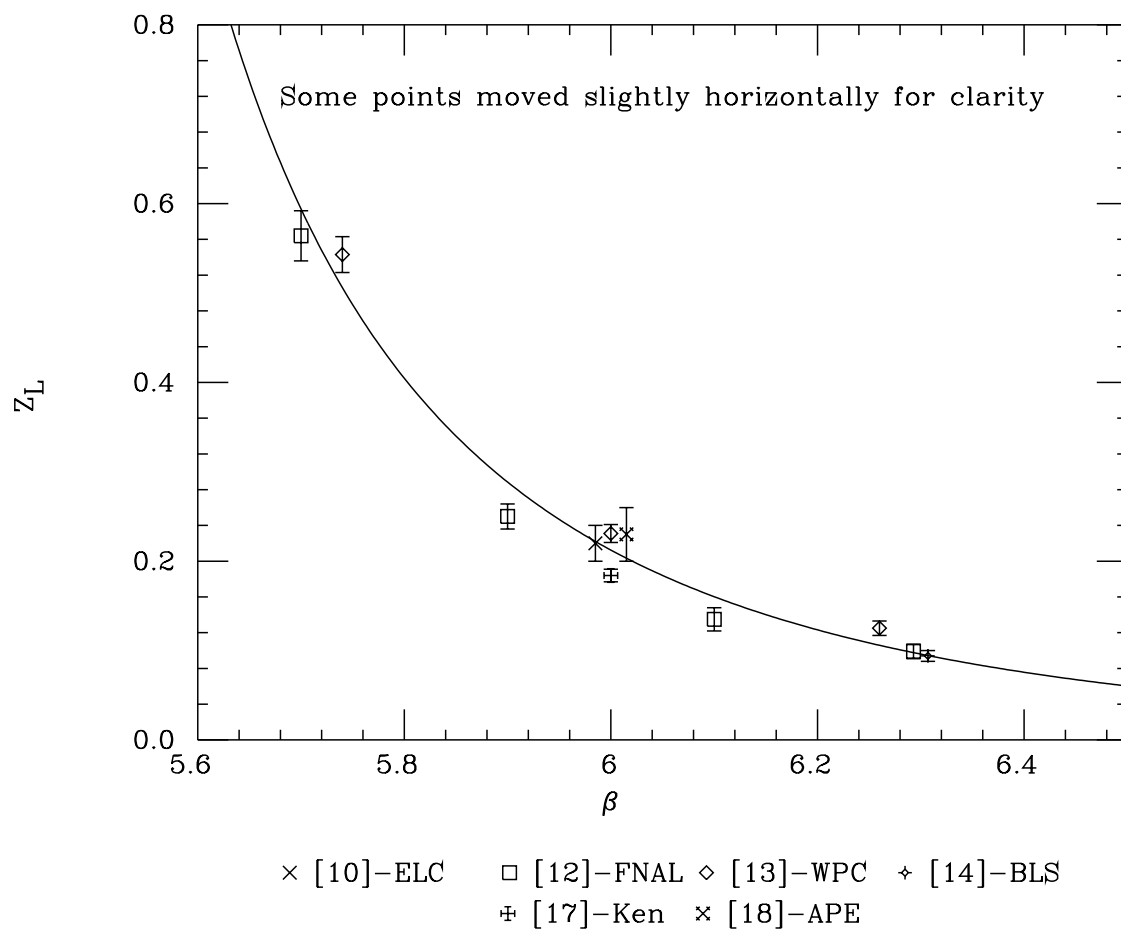


Figure 12: Plot of Z_L against $\beta = 6/g^2$. The solid curve is the fit to eq.(34) (ie. the 2-loop asymptotic scaling formulae with an $O(a)$ term). The references are as appears in the legend. All data is from the Wilson action.